Monitoring forest gross primary productivity with Sentinel-2 using plant trait–based hybrid radiative transfer and machine learning

Carlos Camino
Laboratory of Geo-information Science and Remote Sensing, Wageningen University, Wageningen, The Netherlands
carlos.caminogonzalez@wur.nl

Jose Luis Pancorbo
Institute of BioEconomy (IBE), National Research Council of Italy (CNR), Via Madonna del Piano 10, 50019 Sesto Fiorentino, Italy
joseluis.pancorbodeonate@cnr.it

Lorenzo Genesio
Institute of BioEconomy (IBE), National Research Council of Italy (CNR), Via Madonna del Piano 10, 50019 Sesto Fiorentino, Italy
lorenzo.genesio@ibe.cnr.it

Mirco Migliavacca
Joint Research Centre (JRC), European Commission (EC), Ispra, Italy.
mirco.migliavacca@ec.europa.eu

Pieter Simon Alexander Beck
Joint Research Centre (JRC), European Commission (EC), Ispra, Italy.
Pieter.beck@ec.europa.eu

Jean-Baptiste Féret
TETIS, INRAE, AgroParisTech, CIRAD, CNRS, Université de Montpellier, Montpellier, France
jean-baptiste.feret@teledetection.fr

***Abstract*— Climate change is altering disturbance regimes in European forests, increasing uncertainty in estimates of gross primary productivity (GPP). Here, we present a hybrid framework that combines Sentinel-2 (S2) time series with the PROSAIL radiative transfer model and neural networks to retrieve key plant traits and estimate forest GPP across Europe. A look-up table of 25,000 PROSAIL simulations was generated and spectrally convolved to S2 bands to train neural networks for the inversion of leaf chlorophyll content (Cab) and leaf area index (LAI). Retrieved traits were validated using independent observations from the TRY plant trait database and in situ LAI measurements from the ICOS network .Using the inverted plant traits together with selected structural and red-edge vegetation indices, including a novel continuum-removal red-edge–NIR index (CR-re.nir), we developed a global neural network model to predict GPP at 31 eddy-covariance forest sites, covering evergreen needleleaf, deciduous broadleaf, and mixed forests. The model explains a large fraction of the observed GPP variability (R^2 = 0.86; RMSE ≈ 2.25 µmol CO_2 m^{-2} s^{-1}), demonstrating consistent performance across forest types. The results highlight the value of physically constrained, trait-based approaches for robust and transferable monitoring of forest productivity from Sentinel-2 imagery.**

Keywords—Gross primary productivity, Sentinel-2, PROSAIL, radiative transfer, machine learning, ICOS, chlorophyll, LAI.

I. Introduction

Climate change is intensifying biotic disturbances in forest ecosystems, with direct implications for carbon uptake and land–atmosphere interactions. Gross primary production (GPP) is a key indicator of ecosystem functioning, as it represents the total carbon assimilated through photosynthesis and constitutes the primary input to the terrestrial carbon cycle [1], [2], [3] Variations in GPP directly influence ecosystem respiration, net carbon balance, and climate–carbon feedbacks [4]. However, GPP cannot be directly measured and remains highly uncertain when estimated using terrestrial biosphere models and eddy-covariance–based approaches, particularly across heterogeneous forest ecosystems [5]. Remote sensing offers a unique opportunity to monitor the spatio-temporal variability of forest productivity at regional to global scales [6], [7], yet many existing approaches rely on empirical relationships between spectral indices and GPP that often lack robustness across forest types, canopy structures, and disturbance conditions [8], [9].

II. Data and Methods

A. Eddy-covariance data

We used eddy-covariance (EC) flux data from the ICOS Warm Winter 2020 (WW20) release for the period 2015–2019 [10] for the period 2015-2019. Specifically, we relied on the half-hourly FLUXNET2015_FULLSET_HH_beta-3 product, which is a release of European sites data using the FLUXNET2015 processing workflow (Pastorello et al., 2020). For the subsequent period (2020–2021), not covered by the WW20 release, we relied on half-hourly Level-2 products from the ICOS Ecosystem Thematic Centre (ETC) archive [11]. Specifically, fluxes and meteorological variables were obtained from the FLUXNET_HH product, while leaf area index (LAI) measurements were retrieved from the ANCILLARY_L2 product. The final dataset comprises 31 EC forest sites distributed across Europe, covering a broad range of forest types over the 2015–2021 period.

B. Sentinel-2 time series

For our analysis, we used the SE2 Multispectral time series obtained from the Sentinel-2A and Sentinel-2B satellites. These satellites offered reliable and consistent imaging, with a ten-day revisit time when only Sentinel-2A was operational from July 2015 to mid-2017 for each EC flux tower. Subsequently, the temporal resolution improved to a five-day revisit time following the inclusion of Sentinel-2B. We thereby cover the period from mid 2017 to December 2021 for each EC flux tower. To ensure high-quality data, we applied Level-2A processing to the acquired imagery. The Level-2A processing includes a scene classification layer (SCL) and an atmospheric correction though Sen2Cor algorithm applied to the top-of-atmosphere Level-1C orthoimage products. To ensure spatial consistency among utilized reflectance SE2 bands at 20 meters (B5-B7, B8A, B11, and B12), the visible-NIR SE2 bands (B2-B4, B8, and B9) were resampled to a resolution of 20 meters.

$$CR_{red.nir} = \frac{B_7}{\left(B_{8A}+\left[\frac{(B_5-B_{8A})}{(703.9-864.8)}\right](782.5-864.8)\right)} \tag{1}$$

From the Sentinel-2 imagery, we derived a set of spectral vegetation indices designed to capture variations in canopy structure, chlorophyll content, and leaf water status using visible, near-infrared (NIR), red-edge bands. The complete set of indices, including their mathematical formulations, is summarized in Table I. These indices encompass widely used structural and chlorophyll-sensitive metrics, as well as red-edge indicators specifically selected for their sensitivity to vegetation physiological status and stress. In addition, we introduce a novel continuum-removal red-edge–NIR index (CR-re.nir; Eq. 1) to enhance sensitivity to subtle changes in canopy condition.

TABLE-I. VEGETATION INDICES.

Index	Equation
Structural and GPP-related indices	
TVI	0.5*[120* (B6- B3)-200*(B4-B3)]
EVI	2.5*(B8-B4)/B8+6* B4-7.5*B2+1
NDVIv	[(B8-B4)/ (B8+B4)]*B8
kNDVI	tanh [(B8–B4/ 2(0.5 * B8+ B4) ^2)
Chlorophyll-related indices	
REP	700+40* [(B4+B7)/2 - B5]/(B6-B5)
MCARI2	[1.5*(2.5*(B8-B4)-1.3 * (B8-B3))]/ √ [(2* B8+1)^2-(6*B8-5*√ (B4))-0.5]
IRECI	B7-B4 / (B5/B6)
MTVI1	1.2 *[1.2*(B8-B3)-2.5*(B4-B3)]
MTVI2	[1.5*(1.2*(B8–B3) - 2.5 * (B4-B3))]/√[(2 * B8+1)^2 - (6*B8-5*√(B4))-0.5]
Datt4	B4/(B3*B8)
Red-edge indices	
Chlred.edge	(B7/B5)^-1
CIre	B7/B5-1

C. *Hybrid ML–PROSAIL plant trait retrieval*

We developed a hybrid machine learning–radiative transfer framework to invert Sentinel-2 reflectance and retrieve the key plant traits controlling canopy functioning, namely leaf chlorophyll content (Cab) and leaf area index (LAI). The approach couples neural networks with the PROSAIL-PRO radiative transfer model. A look-up table (LUT) of 25,000 PROSAIL simulations was generated by sampling realistic ranges of pigment content, leaf water content, canopy structure, and viewing–illumination geometry, constrained using field observations, flux data, and literature to avoid ill-posed solutions (Table II). Simulated reflectance spectra were convolved to Sentinel-2 spectral resolution and complemented with red-edge, NIR, and SWIR-based vegetation indices using the ToolsRTM package [12]. For each inverted trait, a three-layer neural network (NN) was trained using PROSAIL-simulated spectra and vegetation indices as predictors. Data balancing, spectral scaling, and additive Gaussian noise were applied during training to improve robustness and generalization to Sentinel-2 observations. Model performance was evaluated using RMSE, MAE, and the coefficient of determination, and the best-performing NN configurations were subsequently used to retrieve Cab and LAI from empirical Sentinel-2 imagery. Cab retrievals were validated using leaf chlorophyll data from the the TRY plant trait database [13], and while LAI estimates were evaluated against in situ measurements from the ICOS Ecosystem Thematic Centre.

D. *Machine learning approach for predicting GPP*

After deriving vegetation indices and plant traits from Sentinel-2 imagery, we used a single neural network model to predict GPP at eddy-covariance flux tower sites. The model combines inverted chlorophyll content and leaf area index with structural, chlorophyll-sensitive, and red-edge vegetation indices (Table I). We developed a global neural network model using all available ICOS forest sites, including evergreen needleleaf, deciduous broadleaf, and mixed forests, with balancing applied to ensure comparable representation of each forest type during model training and evaluation.

TABLE-II. PROSAL LOOK-UP TABLE.

Parameter	Abbreviation	Units	Values
Chlorophyll content	Cab	$\mu g/cm^2$	[0,75]
Carotenoid content	Car	$\mu g/cm^2$	[0,17]
Anthocyanin content	Anth	$\mu g/cm^2$	[0,5]
Water content	EWT	mg/cm^2	[0.1,40]
Leaf proteins	Prot	mg/cm^2	[0.1-5]
Carbon-based const.	CBC	mg/cm^2	[0,20]
Brown pigments	Cbrown	---	[0,1]
Mesophyll struct.	N	---	[1,3]
Leaf area index.	LAI	m^2/m^2	[0.1,7]
Average leaf angle	LIDFa	deg.	[30,90]
Hot spot parameter	Hot	---	[0,0.5]
Observer angle	tto	deg.	[0,15]
Sun zenith angle	tts	deg.	[15,75]
Relative azimuth angle	psi	deg.	[0,130]
Soil factor	psoil	---	[0.25-0.32]

III. RESULTS

The validation results indicate good agreement between plant traits retrieved using the Sentinel-2–PROSAIL framework and independent in situ observations (Fig. 1). Chlorophyll content estimates obtained with the hybrid physically based machine-learning approach show a consistent relationship with leaf chlorophyll measurements from the TRY database ($R^2 = 0.57$; RMSE = 5.02 μg cm^{-2}; MAE = 3.93 μg cm^{-2}), capturing the main variability across sites. Leaf area index (LAI) retrievals exhibit stronger agreement with ICOS field measurements ($R^2 = 0.72$; RMSE = 0.82 m^2 m^{-2}; MAE = 0.69 m^2 m^{-2}), with predictions closely aligned along the 1:1 line.

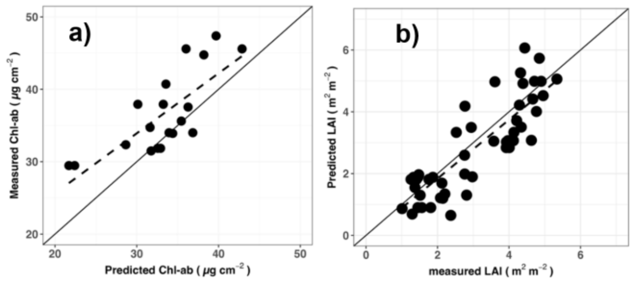

Fig. 1. Validation of Sentinel-2–PROSAIL predictions for chlorophyll content (Chl-ab, μg cm^{-2}) retreived from TRY dataset and leaf area index (LAI, m^2 m^{-2}) measured at ICOS flux towers.

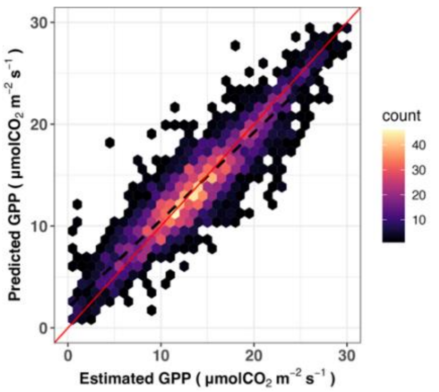

Fig. 2. Validation between flux-derived gross primary productivity (GPP, in μmolCO_2 $m^{-2}s^{-1}$ in black) and neural network–predicted GPP using Sentinel-2–derived plant traits and vegetation indices in the testing dataset.

The neural network model showed strong agreement between predicted and flux-derived GPP across all forest sites (Fig. 2). The model explained a large fraction of the observed variability ($R^2 = 0.86$), with low prediction errors (RMSE = 2.25 μmol CO_2 m^{-2} s^{-1}; MAE = 1.67 μmol CO_2 m^{-2} s^{-1}). The density of points along the 1:1 line indicates a robust and unbiased performance across the full range of GPP values, demonstrating the ability of the trait-based approach to capture both low and high productivity conditions. These results confirm that combining inverted chlorophyll content, leaf area index, and selected structural and red-edge indices provides a reliable framework for estimating forest GPP from Sentinel-2 imagery.

The time series comparison highlights the ability of the hybrid modelling approach to reproduce both the seasonal dynamics and interannual variability of GPP across contrasting forest types (Fig. 3). For both the mixed forest (BE-Vie) and the needleleaf forest (IT-SR2), predicted GPP closely follows flux-derived estimates, capturing periods of increased productivity as well as short-term reductions associated with environmental variability. Minor discrepancies are mainly observed during peak growing-season conditions, but overall the model preserves the timing and magnitude of GPP variations, demonstrating robust performance across forest structures.

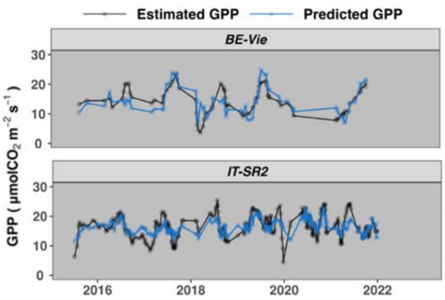

Fig. 3. Time series for the estimates of gross primary productivity (GPP, in μmolCO_2 $m^{-2}s^{-1}$ in black) and predicted GPP uisng an Hybrid modelling approach for a mixed forest site (BE-Vie) and a needleleaf forest site (IT-SR2).

IV. DISCUSSION

The results demonstrate that the proposed hybrid ML–PROSAIL framework can robustly retrieve key plant traits and estimate GPP using a global model trained across multiple forest types, including evergreen needleleaf, deciduous broadleaf, and mixed forests. Despite the structural and biochemical heterogeneity of these ecosystems, the model shows consistent performance, indicating good generalization across contrasting canopy conditions.

The validation of chlorophyll content and LAI confirms that the inverted traits capture the dominant variability relevant for photosynthetic activity. While chlorophyll retrievals exhibit moderate uncertainty, as expected in complex forest canopies, the achieved accuracy is sufficient to support ecosystem-scale GPP modelling. Stronger agreement for LAI highlights the sensitivity of Sentinel-2 red-edge and NIR bands to canopy structure and reinforces the value of combining structural and biochemical traits.

Overall, the good agreement between predicted and flux-derived GPP suggests that a globally trained, trait-based modelling approach provides a reliable and transferable framework for forest productivity monitoring. This hybrid strategy reduces dependence on site-specific calibration and offers a scalable solution for regional-to-continental GPP assessment using Sentinel-2 imagery. Further work should focus on quantifying uncertainties, evaluating vegetation index performance under varying conditions, and assessing sensitivity across forest types.

ACKNOWLEDGMENT

The authors thanks the ICOS Ecosystem Thematic Centre for providing access to eddy-covariance flux and ancillary data. The authors also acknowledge the TRY plant trait database for providing leaf chlorophyll measurements and thank the site principal investigators and technical staff of the ICOS network for maintaining the flux tower observations used in this study.

REFERENCES

[1] F. S. Chapin et al., “Reconciling carbon-cycle concepts, terminology, and methods,” Ecosystems, vol. 9, no. 7, pp. 1041–1050, 2006, doi: 10.1007/s10021-005-0105-7.

[2] C. Beer et al., “Terrestrial Gross Carbon Dioxide Uptake: Global Distribution and Covariation with Climate,” Science (1979), vol. 329, no. 5993, pp. 834 LP – 838, Aug. 2010, doi: 10.1126/science.1184984.

[3] G. B. Bonan, “Forests and climate change: Forcings, feedbacks, and the climate benefits of forests,” Science (1979), vol. 320, no. 5882, pp. 1444–1449, 2008, doi: 10.1126/science.1155121.

[4] S. Piao et al., “Evaluation of terrestrial carbon cycle models for their response to climate variability and to CO2 trends,” Glob Chang Biol, vol. 19, no. 7, pp. 2117–2132, 2013, doi: 10.1111/gcb.12187.

[5] D. Baldocchi, Y. Ryu, and T. Keenan, “Terrestrial Carbon Cycle Variability [version 1 ; referees : 2 approved] Referee Status :,” F1000Res, vol. 5, p. 2371, 2016.

[6] S. W. Running, R. R. Nemani, F. A. Heinsch, M. Zhao, M. Reeves, and H. Hashimoto, “A continuous satellite-derived measure of global terrestrial primary production,” Bioscience, vol. 54, no. 6, pp. 547–560, 2004, doi: 10.1641/0006-3568(2004)054[0547:ACSMOG]2.0.CO;2.

J. Xiao et al., “Remote sensing of the terrestrial carbon cycle: A review of advances over 50 years,” Remote Sens Environ, vol. 233, Nov. 2019, doi: 10.1016/j.rse.2019.111383.

[7] Y. Zhang, J. Joiner, S. Hamed Alemohammad, S. Zhou, and P. Gentine, “A global spatially contiguous solar-induced fluorescence (CSIF) dataset using neural networks,” Biogeosciences, vol. 15, no. 19, pp. 5779–5800, 2018, doi: 10.5194/bg-15-5779-2018.

[8] S. Junttila et al., “Estimating local-scale forest GPP in Northern Europe using Sentinel-2: Model comparisons with LUE, APAR, the plant phenology index, and a light response function,” Science of Remote Sensing, vol. 7, no. October 2022, p. 100075, 2023, doi: 10.1016/j.srs.2022.100075.

[9] Warm Winter 2020 Team, “Warm Winter 2020 ecosystem eddy covariance flux product for 73 stations in FLUXNET-Archive format—release 2022-1 (Version 1.0).,” ICOS Carbon Portal, 2022, doi: https://doi.org/10.18160/2G60-ZHAK.

[10] S. Sabbatini et al., “Eddy covariance raw data processing for CO 2 and energy fluxes calculation at ICOS ecosystem stations,” Int Agrophys, vol. 32, no. 4, pp. 495–515, 2018, doi: 10.1515/intag-2017-0043.

[11] C. Camino, K. Ose, K. Araño, C. Bolyn, and P. S. A. Beck, “RT-Simulator: An Online Platform to Simulate Canopy Reflectance from Biochemical and Structural Plant Properties Using Radiative Transfer Models,” in IGARSS 2024 - 2024 IEEE International Geoscience and Remote Sensing Symposium, 2024, pp. 2811–2814. doi: 10.1109/IGARSS53475.2024.10642442.

[12] J. Kattge et al., “TRY plant trait database – enhanced coverage and open access,” Glob Chang Biol, vol. 26, no. 1, pp. 119–188, Jan. 2020, doi: 10.1111/gcb.14904.